High-Resolution Local Current Measurement of CdTe Solar Cells

Heayoung P. Yoon[1, 3], Dmitry Ruzmetov[1, 3], Paul M. Haney[1], Marina S. Leite[1, 3], Behrang H. Hamadani[2], A. Alec Talin[1], and Nikolai B. Zhitenev[1]

[1]Center for Nanoscale Science and Technology, National Institute of Standards and Technology, Gaithersburg, Maryland, 20899, USA
[2]Energy and Environment Division, National Institute of Standards and Technology, Gaithersburg, Maryland, 20899, USA
[3]Maryland Nanocenter, University of Maryland, College Park, Maryland, 20742, USA

***Abstract* — We investigate local electronic properties of CdTe solar cells using electron beam to excite electron-hole pairs and evaluate spatially resolved photocurrent characteristics. Standard semiconductor processes were used to fabricate Ohmic metal contacts on the surface of *p*-type CdTe / *n*-type CdS device extracted from a commercial solar panel. An ion milling process was used to prepare cross-sections of the devices. Local injection of carriers was controlled by an acceleration voltage of electron beam (1 kV to 30 kV) in a scanning electron microscope, and the results were correlated with the local morphology, microstructure, and chemical composition of the devices.**

***Index Terms* — solar cells, thin film, CdTe, grain boundary, electron beam induced current, EBIC, cross section, focused ion beam.**

I. Introduction

Cadmium Telluride (CdTe) / Cadmium Sulfide (CdS) thin film solar cells are one of the most successful solar energy harvesting technologies on the market today. However, the efficiency of commercial *p*-CdTe / *n*-CdS solar cells is about 13 %, which is well below the theoretical maximum value (≈28 %) possible for this material under 1 sun illumination [1] [2]. The underlying physical mechanisms which limit the efficiency of the CdTe cells are presently not well understood. In particular, variations in local composition and electronic properties of grain bulk, grain surface, and grain boundaries can be important in defining the efficiency of thin film solar cells. Local measurements based on scanning probes or focused electron beams are increasingly used to characterize polycrystalline films. In this work, we use an electron beam to generate carriers locally at grain bulk and grain boundaries, respectively, and the results are correlated with the local morphology, microstructure, and chemical composition of the devices. We also evaluate a possible impact of rough grain morphology and surface processing on the measurements comparing electron beam induced current (EBIC) data obtained on as-prepared, cleaved or polished surfaces and cross-sections. Initial results demonstrating higher collection current at grain boundaries than grain interiors are correlated with other characterizations including cathodoluminescence and local conductivity probe measurements.

II. Experimental

Standard semiconductor processes were used to fabricate Ohmic metal contacts on the surface of *p*-CdTe / *n*-CdS junctions extracted from a commercial solar panel. To fabricate robust and stable contacts on *n*-CdS / TCO (Transparent Conductive Oxide), the top CdTe layer was etched for 10 min in 1% volume fraction of Bromine in methanol solution using a wax mask (petroleum hydrocarbons). The inset of Fig. 1 shows a scanning electron microscopy (SEM) image of selectively etched CdTe layer. A dark current-voltage (*I-V*) characteristic of the device with the fabricated contact (50 nm Au) is shown in Fig. 1.

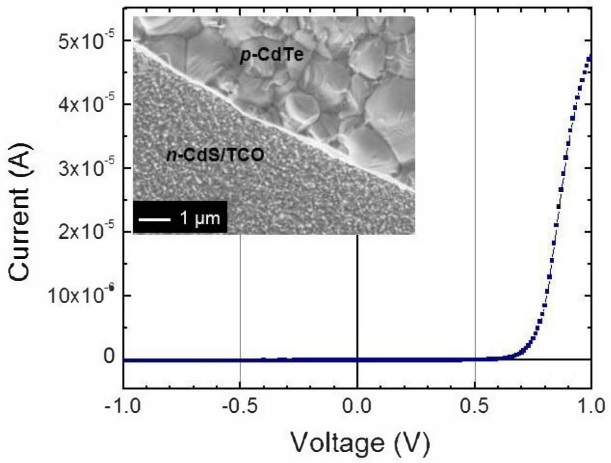

Fig. 1. A dark *I-V* characteristic of *n*-CdS / *p*-CdTe solar cell. The contact metal on CdTe is a 50 nm Au film (300 μm x 500 μm). The inset shows an SEM image of selectively etched CdTe layer prior to Indium soldering to the CdS / TCO.

Cross-sections of the devices were obtained either by cleaving or by a focused ion beam milling (FIB). Acquisition of EBIC images at different electron energy from 1 keV to 30 keV was performed in an SEM system. While the contact of Indium / *n*-CdS / TCO was grounded, a Tungsten probe tip (diameter of 100 nm or 500 nm) controlled by a nanomanipulator was positioned to a desired place on metal / *p*-CdTe. A custom designed sample stage was used to handle

the full range of signals for low- and high keV EBIC with a high signal-to-noise ratio.

III. Results and Discussion

The primary electron beam in a SEM generates electron-hole pairs within an interaction volume in CdTe / CdS devices. The generated carriers drift and diffuse toward the *p-n* junction where they are separated by the internal electrical field. When the contacts on *p*- and *n*- sides are connected in a circuit, the corresponding EBIC current can be measured. EBIC current map reflects the efficiency of carrier collection determined by local built-in and induced electric fields and recombination rates [3].

A series of top-view EBIC images were obtained by varying the acceleration voltage of the electron beam (Fig. 2). Both the number of electron-hole pairs and the penetration depth of electron beam increase at higher electron energies. The energy dependent penetration depth in CdTe was calculated using a Monte-Carlo simulation [4]. Acceleration voltages of 5 kV, 10 kV, and 20 kV generate excitation bulbs of ≈(110 nm)^3, ≈(390 nm)^3, and ≈(1.3 μm)^3, respectively. The carrier collection is the highest when electron beam is positioned at grain boundaries. To evaluate whether the topographic roughness at the grain boundaries can affect the visible EBIC contrast, we also prepare samples by polishing the surface using FIB at low incident angles. The measured EBIC maps are quite similar.

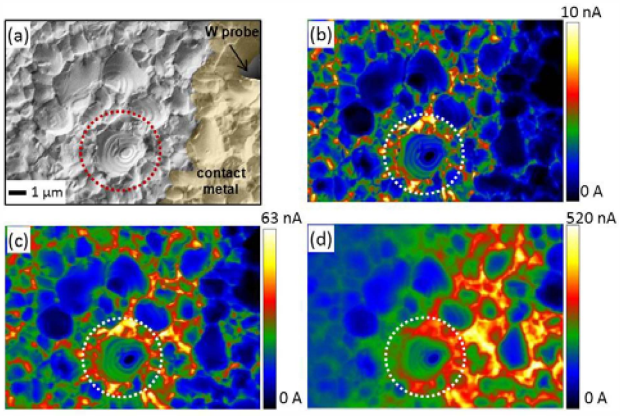

Fig. 2. (a) Top-view SEM image of a small portion of the cell where a probe tip places on a metal contact (*n*-CdS is grounded). Corresponding EBIC images at the acceleration voltage of (b) 5 kV, (c) 10 kV, and (d) 20 kV. Circle indicates a single grain.

In the case of cross-sectional EBIC measurements, *p-n* junctions are perpendicular to the injected of electron beam. The EBIC image is determined by the drift and the diffusion of minority carriers in the internal electric field of the p-n junction. Active defects of the semiconductor devices (e.g., dislocations, impurities) tend to strongly decrease the minority carrier lifetime in their vicinity, resulting in high EBIC signal in defect free areas and weak EBIC signals in areas around such defects.

We prepared cross-sections of *p*-CdTe / *n*-CdS devices either by cleaving or by ion milling. Fig. 3 shows EBIC images at a cleaved edge measured at a tilt angle of 45º. Similarly to the top-view measurements, it appears that the grain boundaries are more efficient in carrier collections than the grain bulk regions, but the jagged broken surface causes difficulties to distinguish the contribution of topography, grain structure and inhomogeneity to the overall EBIC signal.

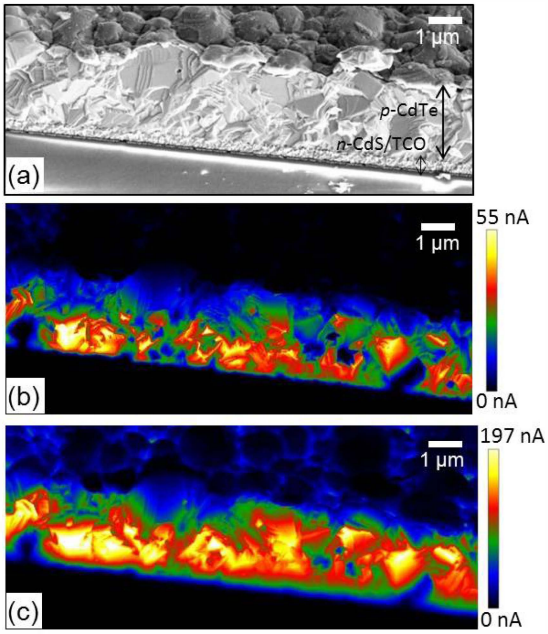

Fig. 3. (a) Cross-sectional SEM image on a cleaved cell (tilt angle of 45º). Corresponding EBIC images at (a) 5 keV and (b) 10 keV.

To gain a better understanding on the local current distribution on the cross-sections, we used a FIB system to fabricate a smooth cross-sectional surface [5]. It is known that Ga ions can penetrate into the material during FIB cross-sectioning, causing distortion of its crystal structure by implanting Ga ions near the surface [6], or accumulate at its surface affecting the recombination of carriers. We carried out a Monte-Carlo simulation [7] to estimate the thickness of the formed amorphous layer, resulting in about 20 nm and 10 nm for perpendicular and gracing incident angle of 30 keV Ga ions, respectively. Ga implantation can also be minimized or avoided using low energy FIB for final polishing [6].

EBIC imaging on the FIB cross-sectioned devices was performed at the acceleration voltage of 1.5 kV (excitation bulb ≈(15 nm)^3 in CdTe), shown in Fig. 4. As expected, the observed EBIC signal is the strongest at the location of *p-n* junction. A line scan in Fig. 4 (b) shows a current decrease on the same grain as the electron beam scans away from the depletion region of *p*-CdTe / *n*-CdS. CdS layer does not show any EBIC activity as reported [8]. Additional, EBIC has

strong maxima at the grain boundaries with amplitudes comparable to these at *p-n* junction. The line scan across single grains in Fig. 4 (c) clearly show a higher EBIC current at grain boundaries than that at grain bulk, consistent with other work [9]. The strong EBIC enhancement can be attributed either to large build-in electric field at the grain boundaries, or to a reduced recombination rate. Details of collection properties of grain boundaries will be further studied using different acceleration voltages and scanning probe-based techniques.

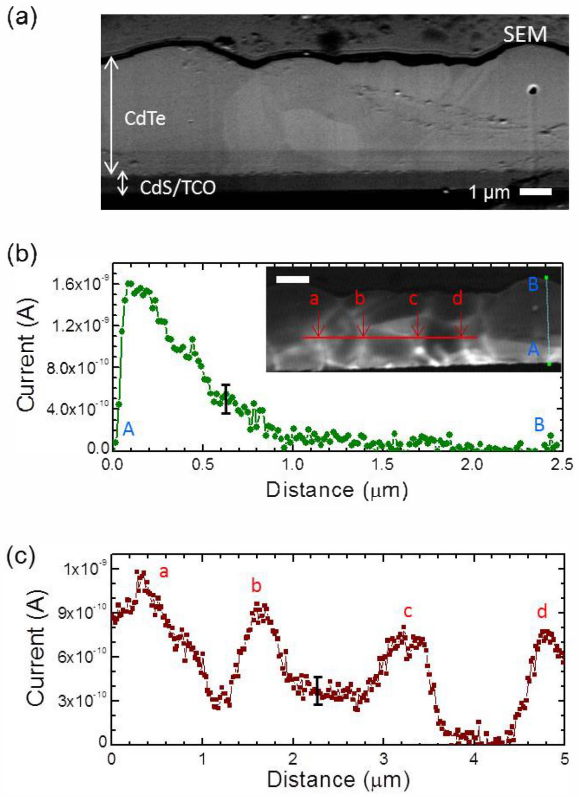

Fig. 4. (a) SEM image after FIB cross-section, (b) Inset shows a 1.5 keV EBIC image obtained at the same position of the cell (tilt angle of 45º, scale bar: 1 µm). Line scan across *n*-CdS / *p*-CdTe junction, (c) Line scan across single grains in *p*-CdTe. Representative error bars indicate one standard deviation uncertainties due to the electrical background noise signal.

IV. Conclusions

We present local electronic properties of polycrystalline CdTe solar cells using electron beams. The generation of electron-hole pairs was estimated using Monte-Carlo simulation. Depth and dimension of depletion region near grain boundary can be visualized by using low acceleration voltage of the electron beams. The measured EBIC currents at grain boundaries were higher than those at grain bulk, indicating that the grain boundaries can be beneficial for improving efficiency of polycrystalline CdTe solar cells under short circuit conditions. In further study, the role of grain boundaries under open circuit conditions will be analyzed, providing deeper insight into a relationship between microstructure and local properties of PV materials.

Acknowledgement

The authors thank Glenn Holland for sample preparations. Also we thank David Gundlach and James Basham for valuable discussions. H. P. Yoon, D. Ruzmetov, M. S. Leite acknowledge support under the Cooperative Research Agreement between the University of Maryland and the National Institute of Standards and Technology Center for Nanoscale Science and Technology, Award 70NANB10H193, through the University of Maryland.

References

[1] R. W. Birkmire, "Pathways to Improved Performance and Processing of CdTe and CuInSe2 Based Modules", in *33th IEEE Photovoltaic Specialist Conference*, 2008, p. 1485.

[2] J. Sites and J. Pan, "Strategies to Increase CdTe Solar Cell Voltage", *Thin Solid Films*, vol. 515, pp. 6099-6102, 2007.

[3] P. R. Edwards, S. A. Galloway, and K. Durose, "EBIC and luminescence mapping of CdTe/CdS solar cells", *Thin Solid Films*, vol. 372, pp. 284-291, 2000.

[4] D. Drouin, A. R. Couture, D. Joly, X. Tastet, V. Aimez, and R. Gauvin, "CASINO V2.42 - A Fast and Easy-touse Modeling Tool for Scanning Electron Microscopy and Microanalysis Users", *Scanning*, vol. 29, pp. 92-101, 2007.

[5] F. Altmann, J. Schischka, N. V. Vinh, S. Stone, L.F.T. Kwakman, L.F.T., R. Lehmann, "Combined Electron Beam Induced Current Imaging (EBIC) and Focused Ion Beam (FIB) Techniques for Thin Film Solar Cell Characterization", in *36th International Symposium for Testing and Failure Analysis*, 2010, p.151.

[6] J. P. Biersack and L. G. Haggmark, "A Monte Carlo Computer Program for the Transport of Energetic Ions in Amorphous Targets", *Nuclear Instruments & Methods*, vol. 174, pp. 257-269, 1980.

[7] D. A. M. De Winter, M. N. Lebbink, D. F. W. De Vries, J. A., Post, M. R. Drury, "FIB-SEM Cathodoluminescence Tomography: Practical and Theoretical Considerations" *Journal of Microscopy*, vol. 243, pp. 315-326, 2011.

[8] R. G. Dhere et al., "Investigation of Junction Properties of CdS/CdTe Solar Cells and Their Correlation to Device Properties", in *33th IEEE Photovoltaic Specialist Conference*, 2008, pp. 1137.

[9] I. Visoly-Fisher, S. R. Cohen, K., Gartsman, K, A. Ruzin, D. Cahen, "Understanding the Beneficial Role of Grain Boundaries in Polycrystalline Solar Cells from Single-Grain-Boundary Scanning Probe Microscopy", *Advanced functional Materials*, vol. 16, pp. 649–660, 2006.